Electronic Supplementary Material (ESI) for Physical Chemistry Chemical Physics.

Supporting Information

Synergistic Theoretical and Experimental Study on Ion Dynamics of Bis(trifluoromethanesulfonyl)imide-based Alkali Metal Salts for Solid Polymer Electrolytes

Brigette Althea Fortuin[1,2,3], Jon Otegi[2], Juan Miguel López del Amo[1], Sergio Rodriguez Peña[1,2], Leire Meabe[1], Hegoi Manzano[2]*, María Martínez-Ibañez[1]*and Javier Carrasco[1,4]*

[1] Centre for Cooperative Research on Alternative Energies (CIC energiGUNE), Basque Research and Technology Alliance (BRTA), Alava Technology Park, Albert Einstein 48, 01510 Vitoria-Gasteiz, Spain
[2] Department of Physics, University of the Basque Country (UPV/EHU), 48940 Leioa, Spain
[3]ALISTORE-European Research Institute, CNRS FR 3104, Hub de l'Energie, Rue Baudelocque, 80039 Amiens Cedex, France
[4] IKERBASQUE, Basque Foundation for Science, Plaza Euskadi 5, 48009 Bilbao, Spain

*Javier Carrasco: E-mail: jcarrasco@cicenergigune.com

*Maria Martinez-Ibañez: E-mail: mmartinez@cicenergigune.com

*Hegoi Manzano: E-mail: hegoi.manzano@ehu.eus

Table S1: Force field parameters for PEO (Figure S4 (a)) including non-bonded parameters; atomic point charges (q), and Lennard-Jones parameters with C_1 and H_1 referring to the terminal methyl groups of the PEO chains; and bonded parameters used in Gromacs[1,2] and LAMMPS[3,4] simulations.

Atom	q (e)	σ (Å)	$\varepsilon\ (kJ\ mol^{-1})$	Bond	r_0 (Å)	k_r $(kJ\ mol^{-1}\ Å^{-2})$	Angle	θ_0 $(degree)$	k_θ $(kJ\ mol^{-1}\ rad^{-2})$
C_1	−0.18	3.50	0.276	C-C	1.529	2242.624	C-C-H	110.7	313.800
H_1	0.06	2.50	0.126	C-H	1.090	2845.120	H-C-H	107.8	276.144
C_2	0.14	3.50	0.276	C-O	1.410	2677.760	H-C-O	109.5	292.880
H_2	0.03	2.50	0.126				C-C-O	109.5	418.400
O	−0.40	2.90	0.586				C-O-C	109.5	502.080
							C-C-C	112.7	488.273

Dihedral	$V_1\ (kJ\ mol^{-1})$	$V_2\ (kJ\ mol^{-1})$	$V_3\ (kJ\ mol^{-1})$	$V_4\ (kJ\ mol^{-1})$
C-C-O-C	1.7154	2.8451	1.0460	−5.6066
H-C-C-H	0.6276	1.8828	0.0	−2.5104
H-C-C-O	0.9791	2.9370	0.0	−3.9162
H-C-O-C	1.5899	4.7698	0.0	−6.3597
O-C-C-O	−1.1506	1.1506	0.0	0.0
C-C-C-H	0.6276	1.8828	0.0	−2.5104
C-C-C-O	2.8744	0.5816	2.0920	−5.5480

Table S2: Force field parameters for XTSFI (Figure S4 (b)) including non-bonded parameters; Lennard-Jones parameters; and bonded parameters used in both GROMACS[1,2,5,6] and LAMMPS simulations[2,5,6].

Atom	σ (Å)	ε ($kJ\ mol^{-1}$l)	Bond	r_0 (Å)	k_r ($kJ\ mol^{-1}$ Å^{-2})	Angle	θ_0 ($degree$)	k_θ ($kJ\ mol^{-1}\ rad^{-2}$)
F	2.95	0.22175	C-F	1.332	3071.056	F-C-F	109.1	644.336
C	3.50	0.27614	C-S	1.770	2845.120	F-C-S	109.5	418.400
S	3.55	1.04600	N-S	1.670	3631.712	C-S-N	103.0	836.800
O	2.96	0.71128	O-S	1.440	5857.600	C-S-O	108.9	619.232
N	3.25	0.71128				N-S-O	107.0	1004.160
Li	2.13	0.07600				O-S-O	119.0	870.232
Na	3.33	0.01598				S-N-S	125.6	671.000
K	4.94	0.00137						
Cs	6.72	0.00034						

Dihedral	V_1 ($kJ\ mol^{-1}$)	V_2 ($kJ\ mol^{-1}$)	V_3 ($kJ\ mol^{-1}$)	V_4 ($kJ\ mol^{-1}$)
F-C-S-N	0.6610	1.9830	0.0000	−2.6440
F-C-S-O	0.7255	2.1765	0.0000	−2.9020
S-N-S-C	45.4636	−36.3221	−18.7348	5.5755
S-N-S-O	−0.0075	−0.0225	0.0000	0.0300
F-C-S-N	0.6610	1.9830	0.0000	−2.6440

Table S3: Lithium-ion molecular speciation as a function of LiTFSI salt concentration.

EO/Li⁺ ratio	Isolated Li^+ (%)	$Li^+ - O^-$ ($TFSI^-$) (%)	$Li^+ - O^-$ (PEO) (%)	$Li^+ - O^-$ ($_{PEO}^{TFSI^-}$) (%)
6:1	0	0.04	76.55	23.44
16:1	0	0	98.05	1.95
20:1	0	0	98.60	1.40
32:1	0	0	99.04	0.96

Table S4: Measured parameters and calculated lithium-ion transference and transport numbers based on EIS and MD, respectively, for PEO_n/LiTFSI SPEs at 70 °C.

EO/Li⁺ ratio	I_i (μA)	I_{ss} (μA)	$R_{Li^+,\,initial}$ (Ω)	$R_{Li^+,\,ss}$ (Ω)	ΔV (mV)	$T_{Li^+}^{EIS}$	$t_{Li^+}^{MD}$
6:1	2	9	313	348	10	0.16 ± 0.025	0.22
16:1	4	2	201	193		0.22 ± 0.024	0.31
20:1	145	67	43	40		0.24 ± 0.024	0.31
32:1	83	37	101	107		0.22 ± 0.026	0.30
64:1	105	51	53	32		0.26 ± 0.025	-

Table S5: Thermal properties of neat PEO and PEO_n/LiTFSI SPEs.

EO/Li⁺ ratio	T_g (°C)	T_m (°C)	ΔH_m (J g^{-1})	χ_c
Neat PEO	–	67	117	57
6:1	−26	55	3	6
16:1	− 35	49	52	36
20:1	− 35	55	70	45
32:1	− 43	56	84	49
64:1	–	62	104	56

Table S6: Raman Spectroscopy peak deconvolution analysis as a function of temperature and LiTFSI salt concentration.

EO/Li⁺ ratio	***25*** °C ***(non-preheated)***		***40*** °C		***70*** °C	
	Dissociated LiTFSI (%)	Associated LiTFSI (%)	Dissociated LiTFSI (%)	Associated LiTFSI (%)	Dissociated LiTFSI (%)	Associated LiTFSI (%)
6:1	90	10	85	15	77	23
16:1	100	0	93	7	96	4
20:1			100	0	100	0
32:1			100	0	100	0
64:1			100	0	100	0

Table S7: Linewidth, chemical shifts, and deconvolution values of the ^{7}Li MAS-NMR spectra from Figure 4. Narrower components are highlighted in orange, while broader components are highlighted in white.

Temperature (°C)	Linewidth (Hz)		Chemical shift (ppm)		Deconvoluted spectra (%)	
	PEO_6/LiTFSI	PEO_{32}/LiTFSI	PEO_6/LiTFSI	PEO_{32}/LiTFSI	PEO_6/LiTFSI	PEO_{32}/LiTFSI
40	12	15	−1.37	−1.45	47	46
	365	167	−1.23	−1.54	53	54
50	9	12	−1.35	−1.44	43	48
	175	70	−1.34	−1.48	56	52
60	7	10	−1.35	−1.42	36	63
	84	39	−1.35	−1.44	64	38
70	6	9	−1.35	−1.41	32	100
	40		−1.36		68	0
80	6	9	−1.34	−1.40	33	100
	28		−1.34		67	0

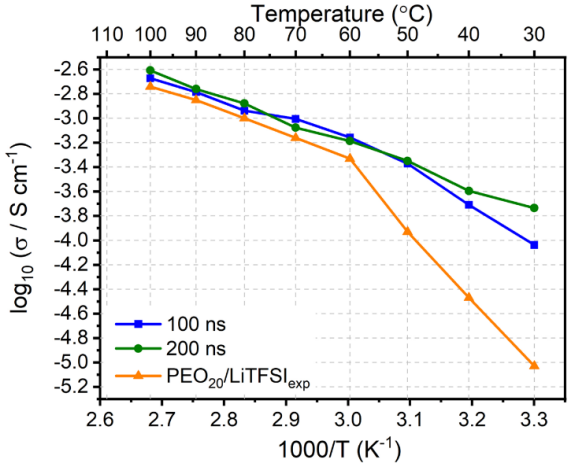

Figure S1: Ionic conductivity of PEO_{20}/LiTFSI simulated for 100 and 200 ns, compared to experimental values obtained from literature[7].

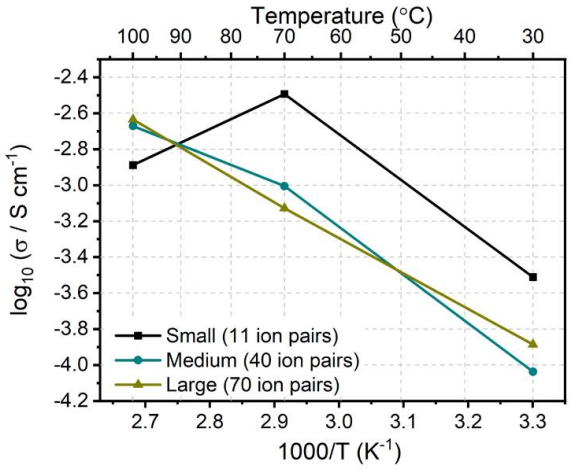

Figure S2: Ionic conductivity of PEO_{20}/LiTFSI at different temperatures for three simulation box sizes: small (11 ion pairs), medium (40 ion pairs), and large (70 ion pairs).

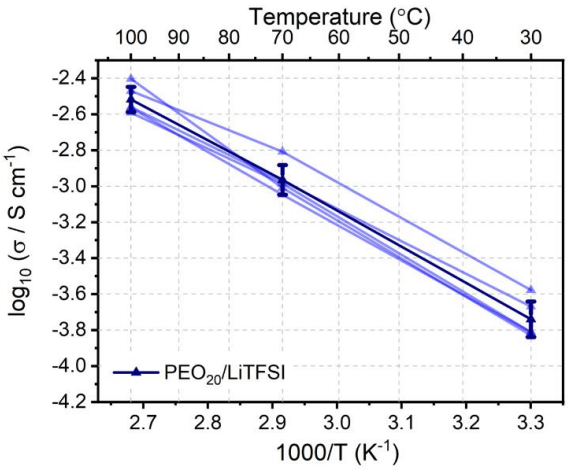

Figure S3: Ionic conductivity of PEO_{20}/LiTFSI at different temperatures with different initial conditions modelled with a medium sized simulation box. The error for the ionic conductivity at each studied temperature is ~ 30 %.

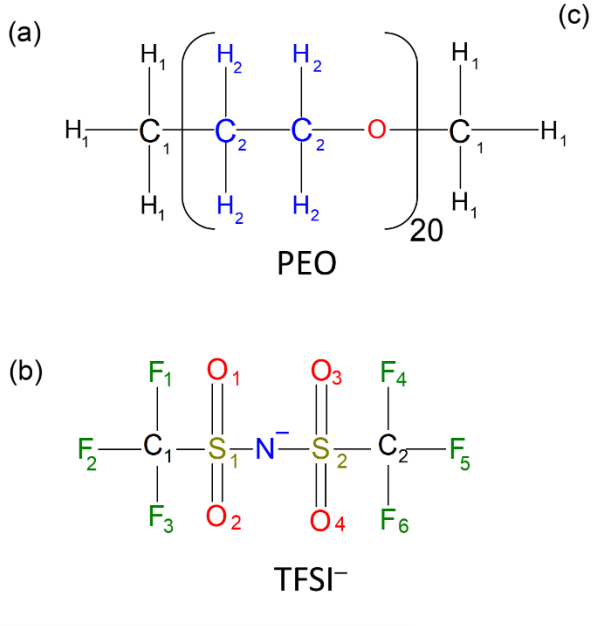

(c)

Atomic charges of $TFSI^-$

Atom	Charge (q) / e
C_1	0.0311
F_1	–0.0507
F_2	–0.0445
F_3	–0.0496
S_1	0.5046
O_1	–0.2940
O_2	–0.3030
N	–0.2987
S_2	0.5475
O_3	–0.2930
O_4	–0.3164
C_2	–0.0380
F_4	–0.0164
F_5	–0.0359
F_6	–0.0430

Figure S4: Chemical structures of (a) PEO and (b) $TFSI^-$ with the corresponding adopted acronyms, and (c) the atomic charges of each atom found in $TFSI^-$, utilized in MD simulations (Tables S1 – S2).

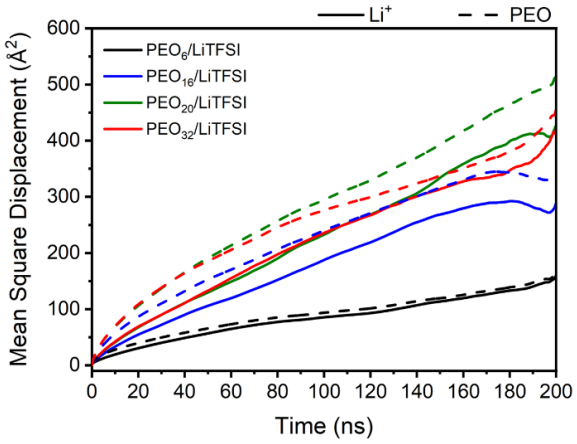

Figure S5: Mean square displacement functions of lithium-ions (solid line) and PEO (dashed line) as a function of LiTFSI salt for the studied PEO_n/LiTFSI SPEs, where n = 6, 16, 20, or 32.

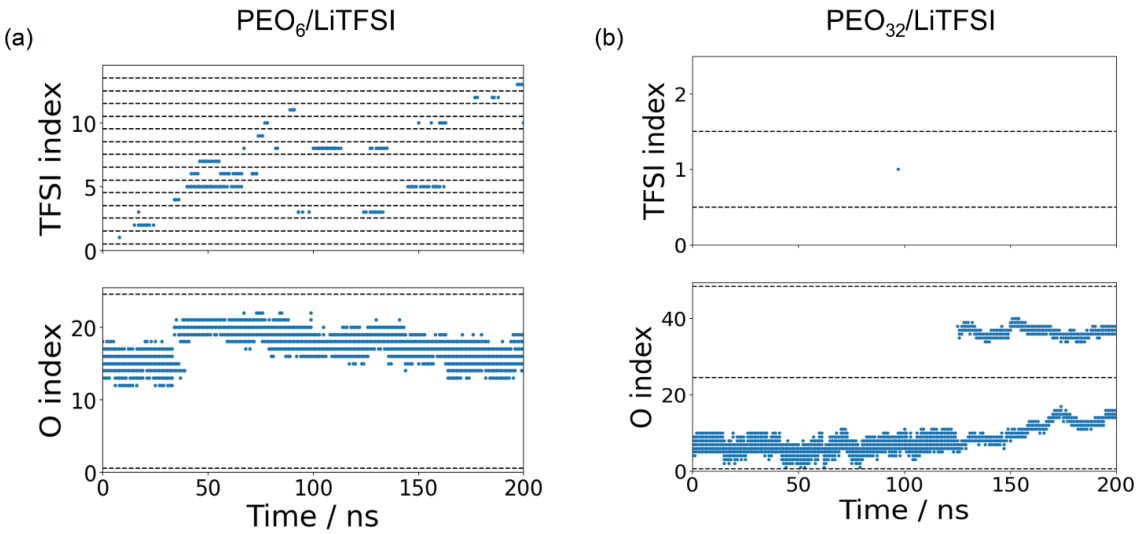

Figure S6: Lithium-ion transport mechanism utilizing a single lithium-ion as reference particle, for (a) PEO_6/LiTFSI and (b) PEO_{32}/LiTFSI. The O index represents the number of oxygens from PEO the lithium-ion interacts with, and the TFSI index represents the number of oxygen atoms from $TFSI^-$ ions the lithium-ion interacts with, over the total simulation time of 200 ns. The delineated dashed line signifies the separation between either one $TFSI^-$ ion from the next, or one PEO chain from the next.

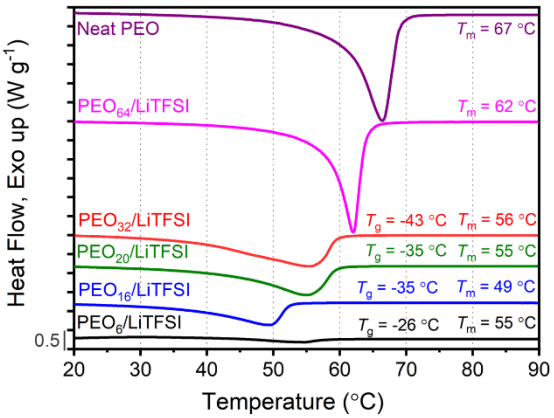

Figure S7: DSC traces of neat PEO (purple) and studied PEO_n/LiTFSI SPEs, where n = 6 (black), 16 (blue), 20 (green), 32 (red), or 64 (magenta).

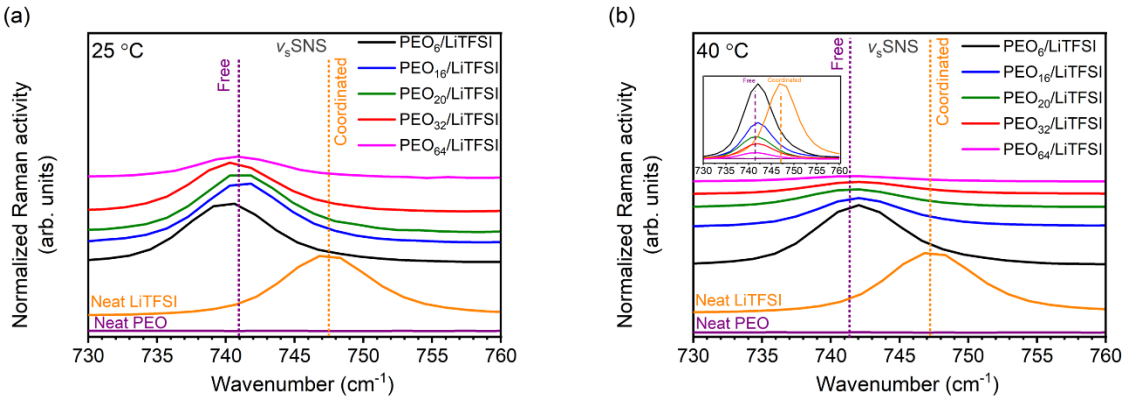

Figure S8: Raman spectra of the 760 - 730 cm^{-1} vibrational window illustrating the *S—N—S* vibration for PEO$_n$/LiTFSI SPEs at (a) 25 °C, and (b) 40 °C, with spectra of neat LiTFSI and neat PEO recorded at 25 °C. The two vertical dotted lines correspond to the coordinated contact ion pair position at 747 cm^{-1} (orange) and the free ion pair position at 740 cm^{-1} (purple), respectively.

Activation energies of the transport mechanisms

Activation energies were calculated by fitting the MD simulated ionic conductivity results to the Arrhenius equation, equation S1:

$$\sigma = Ae^{-\frac{E_A}{k_B T}} \quad \text{(S1)}$$

Upon linearization of equation S1, equation S2 is plotted as shown in Figure S9:

$$ln\sigma = \ln A - \frac{E_A}{k_B \times T} \quad \text{(S2)}$$

By performing a linear regression of the natural logarithm of the ionic conductivity versus the inverse of the temperature, the activation energy may be deduced from the slope (cf. Table S8).

Table S8: Activation energies (along with the R^2 values of the fitting to the Arrhenius equation) for the studied PEO$_{20}$/XTFSI systems, where X = Li, Na, K, and Cs.

Cation	E_A (eV)	R^2
Li$^+$	0.1837	0.9629
Na$^+$	0.1579	0.9812
K$^+$	0.1582	0.9947
Cs$^+$	0.1816	0.9564

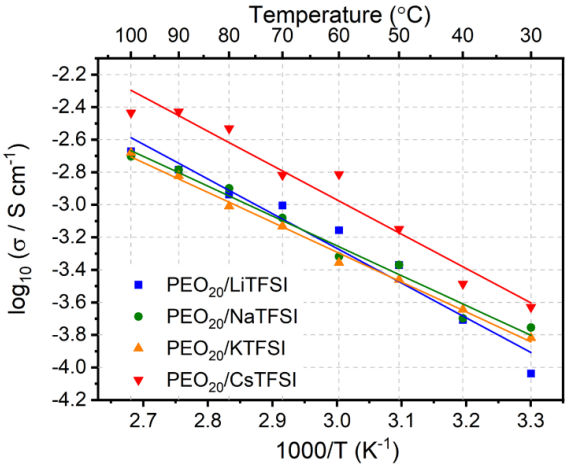

Figure S9: Linearized fitting of the ionic conductivity for the studied PEO$_{20}$/XTFSI systems; with lithium (blue), sodium (green), potassium (orange), and cesium (red) cations.

REFERENCES

1 S. Pronk, S. Páll, R. Schulz, P. Larsson, P. Bjelkmar, R. Apostolov, M. R. Shirts, J. C. Smith, P. M. Kasson, D. Van Der Spoel, B. Hess and E. Lindahl, GROMACS 4.5: A high-throughput and highly parallel open source molecular simulation toolkit, *Bioinformatics*, 2013, **29**, 845–854.

2 L. Meabe, S. R. Peña, M. Martinez-Ibañez, Y. Zhang, E. Lobato, H. Manzano, M. Armand, J. Carrasco and H. Zhang, Insight into the ionic transport of solid polymer electrolytes in polyether and polyester blends, *Journal of Physical Chemistry C*, 2020, **124**, 17981–17991.

3 N. Kondratyuk, V. Nikolskiy, D. Pavlov and V. Stegailov, GPU-accelerated molecular dynamics: State-of-art software performance and porting from Nvidia CUDA to AMD HIP, *Int J High Perform Comput. Appl*, 2021, **35**, 312–324.

4 C. Kutzner, S. Páll, M. Fechner, A. Esztermann, B. L. de Groot and H. Grubmüller, More bang for your buck: Improved use of GPU nodes for GROMACS 2018, *J Comput. Chem*, 2019, **40**, 2418–2431.

5 A. S. L. Gouveia, C. E. S. Bernardes, L. C. Tomé, E. I. Lozinskaya, Y. S. Vygodskii, A. S. Shaplov, J. N. C. Lopes and I. M. Marrucho, Ionic liquids with anions based on fluorosulfonyl derivatives: from asymmetrical substitutions to a consistent force field model, *Physical Chemistry Chemical Physics*, 2017, **19**, 29617–29624.

6 J. N. Canongia Lopes and A. A. H. Pádua, CL&P: A generic and systematic force field for ionic liquids modeling, *Theor Chem Acc*, 2012, **131**, 1129.

7 U. Oteo, M. Martinez-Ibañez, I. Aldalur, E. Sanchez-Diez, J. Carrasco, M. Armand and H. Zhang, Improvement of the Cationic Transport in Polymer Electrolytes with (Difluoromethanesulfonyl)(trifluoromethanesulfonyl)imide Salts, *ChemElectroChem*, 2019, **6**, 1019–1022.